Entanglement and quantum superposition induced by a single photon

Xin-You Lü,* Gui-Lei Zhu, Li-Li Zheng, and Ying Wu†
School of Physics, Huazhong University of Science and Technology, Wuhan 430074, China

(Received 28 September 2017; published 8 March 2018)

We predict the occurrence of single-photon-induced entanglement and quantum superposition in a hybrid quantum model, introducing an optomechanical coupling into the Rabi model. Originally, it comes from the photon-dependent quantum property of the ground state featured by the proposed hybrid model. It is associated with a single-photon-induced quantum phase transition, and is immune to the A^2 term of the spin-field interaction. Moreover, the obtained quantum superposition state is actually a squeezed cat state, which can significantly enhance precision in quantum metrology. This work offers an approach to manipulate entanglement and quantum superposition with a single photon, which might have potential applications in the engineering of new single-photon quantum devices, and also fundamentally broaden the regime of cavity QED.

DOI: 10.1103/PhysRevA.97.033807

I. INTRODUCTION

Entanglement and quantum superposition, as the fundamental concepts of quantum mechanics, have wide applications in modern quantum technologies [1,2]. Ground-state entanglement and quantum superposition are usually connected with a quantum phase transition (QPT) in strongly correlated quantum systems [3–8]. The Dicke model, describing a system of quantized single-mode cavity fields uniformly coupled to N two-level systems, predicts an equilibrium superradiant QPT in the thermodynamic limit $N \to \infty$, i.e., the phase transition from a normal phase (NP) to a superradiant phase (SP) as increasing the spin-field coupling strength [9]. Different from the Dicke model, the Rabi model considers a system composed of a quantized single-mode field (with frequency ω) coupled to a single two-level system (with transition frequency Ω), which is far from being in the thermodynamic limit. However, it is shown that an equilibrium superradiant QPT also exists in the Rabi model, when the ratio of Ω to ω approaches infinity, i.e., the classical oscillator limit $\Omega/\omega \to \infty$ [10,11]. Associating with the superradiant QPT, the critical entanglement phenomenon [6,7] and quantum superposition of fields [8] could be realized in cavity QED systems. However, they are limited by the so-called A^2 term of the spin-field interaction, which corresponds to the debate on the existence of an equilibrium superradiant QPT in cavity and circuit QED systems [12–18].

Recent advances in materials science and nanofabrication have led to spectacular achievements in single-photon technologies, including single-photon generation in cold atoms [19,20], quantum dots [21–23], diamond color centers [24], or superconducting circuits [25], and single-photon detection based on quantum entanglement [26] or cross-phase modulation [27–29], etc. These achievements have potential applications in quantum information science [30], which has led to the recent explorations of single-photon transistors [31], single-photon routers [32], single-photon switches [33], and single-photon triggered single-phonon sources [34].

To combine the single-photon technologies with entanglement and quantum superposition, here we investigate the ground-state property of a hybrid quantum model, i.e., a Rabi model coupled to an ancillary cavity mode via a quadratic optomechanical coupling. Cavity optomechanics is a rapidly developing research field exploring nonlinear photon-phonon interactions [35–38]. Typically, the quadratic optomechanical coupling strength is very weak [39,40], which limits its application in the quantum realm [41]. Recent proposals have shown that it might be increased by a measurement-based method [42], near-field effects [43], good tunability of the superconducting circuit [44], or modulation of the photon-phonon interaction [45].

Interestingly, the concepts of single-photon-induced entanglement and quantum superposition are proposed in the hybrid quantum model. Physically, the proposed quantum model has a photon-dependent quantum property of the ground state, which corresponds to a single-photon-induced superradiant QPT both in the cases of ignoring and including the A^2 term. This ultimately leads to the realizations of single-photon-induced entanglement and quantum superposition even in the weak-coupling regime of the spin-field interaction, and it is immune to the A^2 term. In general, the realizations of ground-state entanglement and quantum superposition in normal cavity QED systems are limited by the A^2 term. Moreover, here one can obtain a squeezed cat state of field, which could be used to enhance the detection precision in quantum metrology [46,47]. This unconventional single-photon-induced entanglement and quantum superposition is not only fundamental interesting, but can also inspire the engineering of new single-photon quantum devices.

II. MODEL

We consider a hybrid quantum model depicted in Fig. 1(a) with a total Hamiltonian ($\hbar = 1$)

$$H = H_{\rm an} + H_{\rm rm} - g_0 a^\dagger a (b^\dagger + b)^2, \tag{1}$$

*xinyoulu@hust.edu.cn
†yingwu2@126.com

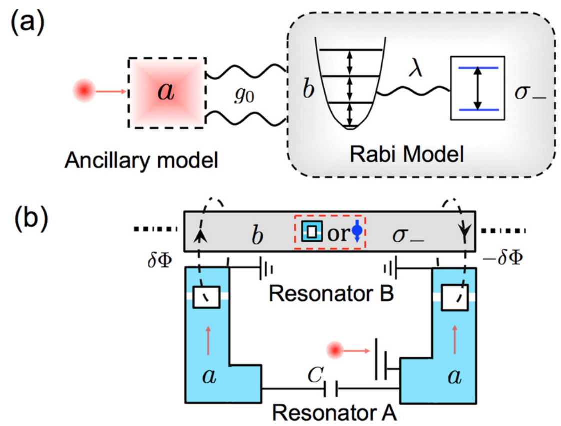

FIG. 1. (a) A hybrid quantum model including a Rabi model quadratically coupled to an ancillary cavity mode a with coupling strength g_0. (b) The implementation of this model in a superconducting circuit with the ability of simulating a quadratic optomechanical coupling [44] and coupling to a superconducting qubit or spin [49].

where a ($a^\dagger$) and b ($b^\dagger$) are the annihilation (creation) operators of the ancillary cavity mode and the field mode of the Rabi model, respectively. The Hamiltonian $H_{\rm rm}$ is given by $H_{\rm rm} = (\Omega/2)\sigma_z + \omega b^\dagger b - \lambda(b^\dagger + b)\sigma_x + (\alpha\lambda^2/\Omega)(b^\dagger + b)^2$, where σ_z and σ_x are the Pauli operators for the two-level system. It describes a two-level system σ_- coupled to a field mode b with coupling strength λ, and the A^2 term has been included in the last term. Normally, $\alpha \geqslant 1$ (decided by the Thomas-Reiche-Kuhn sum rule [14]) corresponds to the case of implementing the Rabi model in a cavity QED system, and $H_{\rm rm}$ is reduced to the Hamiltonian of a standard Rabi model when $\alpha = 0$. The ancillary cavity, with Hamiltonian $H_{\rm an} = \omega_a a^\dagger a$, quadratically couples to b with coupling strength g_0 [40]. This quadratic term provides a photon-dependent modification on the potential of field b. In the classical limit of the ancillary mode a, this model is approximately equivalent to the model studied in Ref. [48], where a time-dependent driving magnitude is employed. Here, we consider the case of a being in a quantum state, i.e., Fock state $|n\rangle_a$, which allows for the occurrence of single-photon-induced entanglement and quantum superposition. Moreover, the interplay between this quadratic interaction and the A^2 term is considered in our work, which makes our results immune to the A^2 term. Here, we denote $|\uparrow\rangle, |\downarrow\rangle$ as the eigenstates of σ_z, and $|m\rangle_b$ as the eigenstate of $b^\dagger b$. Hamiltonian (1) has $\mathbb{Z}_2$ symmetry associating with a well-defined parity operator $\Pi = e^{i\pi\mathcal{N}}$ (i.e., $[\Pi, H] = 0$), where $\mathcal{N} = b^\dagger b + (1/2)(\sigma_z + 1)$ is the total excitation number of the system (excluding the ancillary cavity).

In principle, the proposed hybrid model could be realized in a quadratically coupled optomechanical system with a "membrane-in-the-middle" configuration. However, the typical quadratic coupling in the optomechanical system is too weak. It might be enhanced by driving the mechanical system to large occupation numbers, but too strong driving will make the small displacement approximation used to derive the optomechanical interaction ineffective. Here, we suggest to use the superconducting circuit depicted in Fig. 1(b) to implement our model. Specifically, as shown in Ref. [44], the coupling capacitor C and the superconducting quantum interference devices (SQUIDs) forming resonator A offer an effective fixed semitransparent membrane and movable cavity ends, respectively. A relative displacement of the fixed membrane with respect to the center of resonator A is generated by synchronizing the motion of the movable cavity ends, which is obtained by applying opposite flux variations $\pm\delta\Phi$ through the SQUIDs. Then, the position quadrature of resonator B couples quadratically to the photon number of resonator A in a certain regime. Associating with the interaction between the circuit cavity and the superconducting qubit or spin [49], our model could be realized in a superconducting circuit shown in Fig. 1(b), in which enough large g_0/ω might be reached in the further experiments by optimizing the coupling capacitance C, the bias flux through the SQUIDs, and the geometrical arrangement of the circuit [44].

III. PHOTON-DEPENDENT GROUND-STATE QPT

Considering the ancillary mode a is prepared into a Fock state $|n\rangle_a$ ($n = 0,1,\ldots$), the number operator $a^\dagger a$ can be replaced by an algebraic number n. Then, applying a squeezing transformation $b = \cosh(r_n)b_n + \sinh(r_n)b_n^\dagger$ with $r_n = (-1/4)\ln[1 + \alpha\chi^2 - 4ng_0/\omega]$ and a rescaled coupling strength $\chi = 2\lambda/\sqrt{\Omega\omega}$, the Hamiltonian (1) becomes

$$H_n = \frac{\Omega}{2}\sigma_z + \omega_n b_n^\dagger b_n - \lambda_n(b_n^\dagger + b_n)\sigma_x + C_n, \qquad (2)$$

where $\omega_n = \exp(-2r_n)\omega$, $\lambda_n = \exp(r_n)\lambda$, and $C_n = n\omega_a + [\exp(-2r_n) - 1](\omega/2)$. It clearly shows that the proposed model is essentially equivalent to a photon-dependent Rabi model.

In the $\Omega/\omega \to \infty$ limit (corresponding to $\Omega/\omega_n \to \infty$), Hamiltonian (2) can be diagonalized analytically (see the Appendix). A photon-dependent quantum critical point $\chi_n = 2\lambda_n/\sqrt{\Omega\omega_n} = 1$ is obtained, corresponding to $\chi = \exp(-2r_n) = \sqrt{1 + \alpha\chi^2 - 4ng_0/\omega}$ in terms of the original system parameters. When $\chi < \exp(-2r_n)$, the system is in the NP, featured by an excitation energy ω_e. The ground state of the system is $|G\rangle_{\rm np}$, and it has a conserved $\mathbb{Z}_2$ symmetry (i.e., $\Pi|G\rangle_{\rm np} = |G\rangle_{\rm np}$), confirmed by the zero ground-state coherence of field $\langle b\rangle_g = 0$. The excitation energy ω_e vanishes when $\chi = \exp(-2r_n)$, locating the superradiant QPT. When $\chi > \exp(-2r_n)$, the system enters into the SP and has an excitation energy $\tilde{\omega}_e$. Now the ground state of the system becomes twofold degenerate, i.e., $|G\rangle_{\rm sp}^{\pm}$ (the detailed expression shown in the Appendix). It corresponds to a spontaneous $\mathbb{Z}_2$ symmetry breaking (i.e., $\Pi|G\rangle_{\rm sp}^{+} = |G\rangle_{\rm sp}^{-}$), as is evident from the nonzero ground-state coherence of field $\langle b\rangle_g^{\pm} = \pm\exp(r_n)\beta$. The rescaled ground-state occupation of field b, i.e., $\psi_{\rm q} = [\exp(-4r_n)\omega/\Omega]\langle b^\dagger b\rangle_g$, can be defined as the order parameter characterizing this superradiant QPT. Because $\psi_q = 0$ when $\chi < \exp(-2r_n)$, $\psi_{\rm q} = (1/4)(\chi_n^2 - \chi_n^{-2})$ becomes finite when $\chi > \exp(-2r_n)$, which is clearly displayed by the solid lines of Figs. 2(a)–2(c).

Interestingly, the above photon-dependent quantum criticality leads to a single-photon-induced QPT, when we focus on the cases of $n = 0,1$. Specifically, when the ancillary mode a is in the vacuum state $|0\rangle_a$, Hamiltonian (2) is reduced to a standard Rabi Hamiltonian. The superradiant QPT occurs at $\chi = 1$ when $\alpha = 0$, and it is prevented when $\alpha \geqslant 1$ due to the

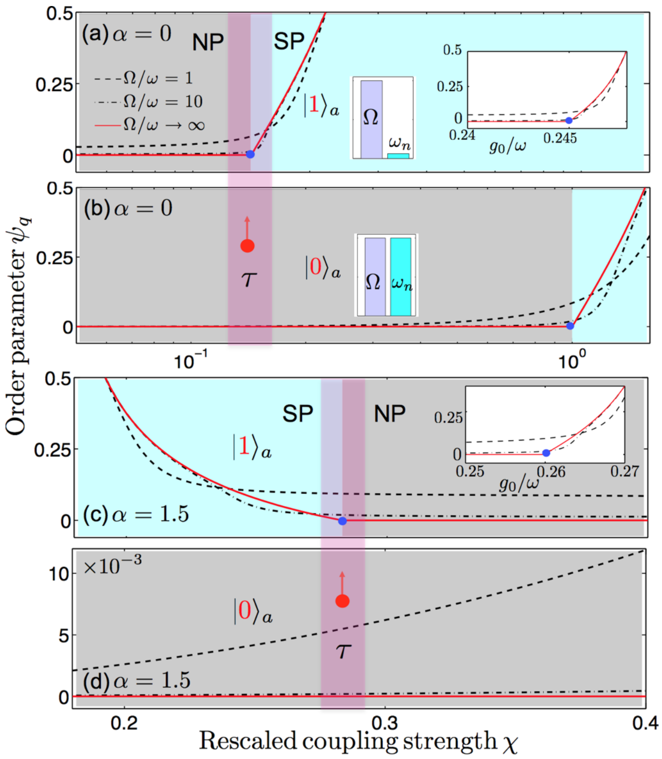

FIG. 2. The order parameter ψ_q vs χ (and g_0/ω in the insets) for different Ω/ω when (a), (b) $\alpha = 0$ and (c), (d) $\alpha = 1.5$. The bar graphs in the insets present Ω/ω_n when mode a is in $|0\rangle_a, |1\rangle_a$, and $\Omega = \omega$. The blue dots indicate the quantum critical point, where ψ_q becomes finite from zero. The pink shaded areas indicate the parameter range τ used to demonstrate single-photon-induced QPT. The system parameters are chosen as (a), (b) $g_0/\omega = 0.245$ and (c), (d) $g_0/\omega = 0.26$.

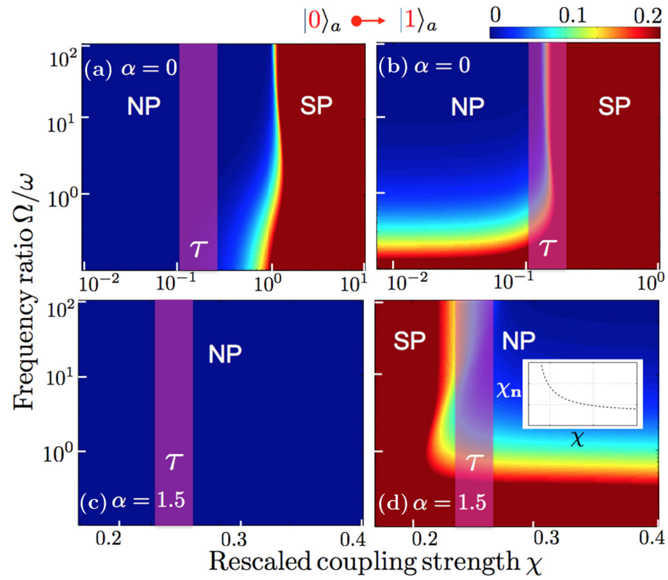

FIG. 3. The order parameter ψ_q vs χ and Ω/ω when (a), (b) $\alpha = 0$, and (c), (d) $\alpha = 1.5$. (a), (c) and (b), (d) correspond to mode a being in the Fock states $|0\rangle_a$ and $|1\rangle_a$, respectively. The inset of (d) presents the dependence of χ_n on χ, and the system parameters are the same as in Fig. 2.

no-go theorem [10]. When a is in the single-photon Fock state $|1\rangle_a$, the superradiant QPT occurs at $\chi = \exp(-2r_1)$, which could be much smaller than 1 for both cases of $\alpha = 0$ and $\alpha \geqslant 1$, by properly choosing the system parameters. Let us consider a parameter range $\chi \in \tau$ to check the occurrence of the superradiant QPT (τ covering the single-photon-induced quantum critical point, $\chi = e^{-2r_1}$). As shown in Fig. 2, in $\Omega/\omega \to \infty$, the superradiant QPT during τ is triggered by exciting a single photon in mode a (i.e., $|0\rangle_a \to |1\rangle_a$). It corresponds to a single-photon-induced $\mathbb{Z}_2$ symmetry breaking, demonstrated by the ground-state coherence of field $\langle b\rangle_g$. Note that this QPT describes the sudden change in the ground state in a closed system as changing the system parameter χ at zero temperature. It belongs to the equilibrium phase transition [9,10], which is different from the nonequilibrium phase transition characterized by the steady state of the driven open systems [50–52].

Including the A^2 term, this superradiant QPT can still occur, since the parameter condition $\chi > \exp(-2r_1)$ can be satisfied even when $\alpha \geqslant 1$. Moreover, the present superradiant QPT is reversed compared with the case in a standard Rabi model [10], i.e., the transition from the NP to the SP occurs as decreasing the original system parameter χ, as shown in Fig. 2(c). This originally comes from the competition between the quadratic term and the A^2 term in Hamiltonian (1), which ultimately leads to the result that χ_n increases along with decreasing χ [see the inset of Fig. 3(d)].

In finite Ω/ω (corresponding to finite Ω/ω_n), the dependence of the order parameter ψ_q on χ (or g_0/ω) clearly approaches the case of a QPT occurring exactly with increasing Ω/ω (see Figs. 2 and 3). This tendency could be faster when $n = 1$, compared with the case of $n = 0$. Physically, in our model, a single photon can induce a dramatic increase in the

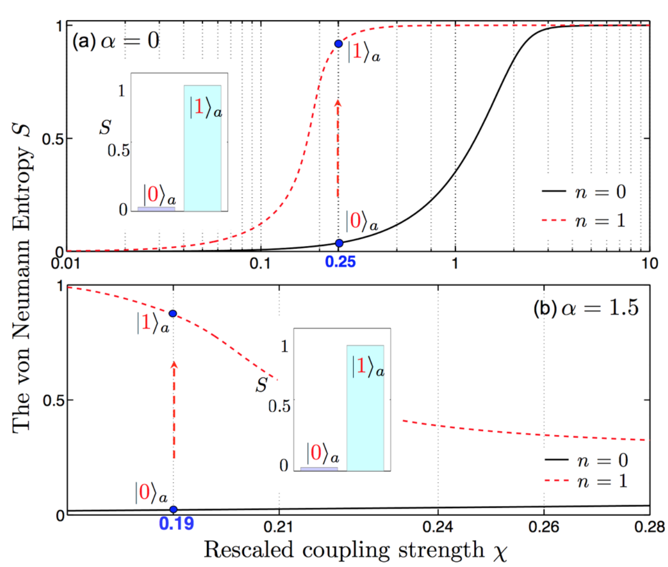

FIG. 4. The von Neumann entropy S vs χ for different n when (a) $\alpha = 0$ and (b) $\alpha = 1.5$. The insets indicate the values of S corresponding to the blue dots. The red dashed arrows indicate single-photon-induced quantum entanglement. The system parameters are the same as in Fig. 2.

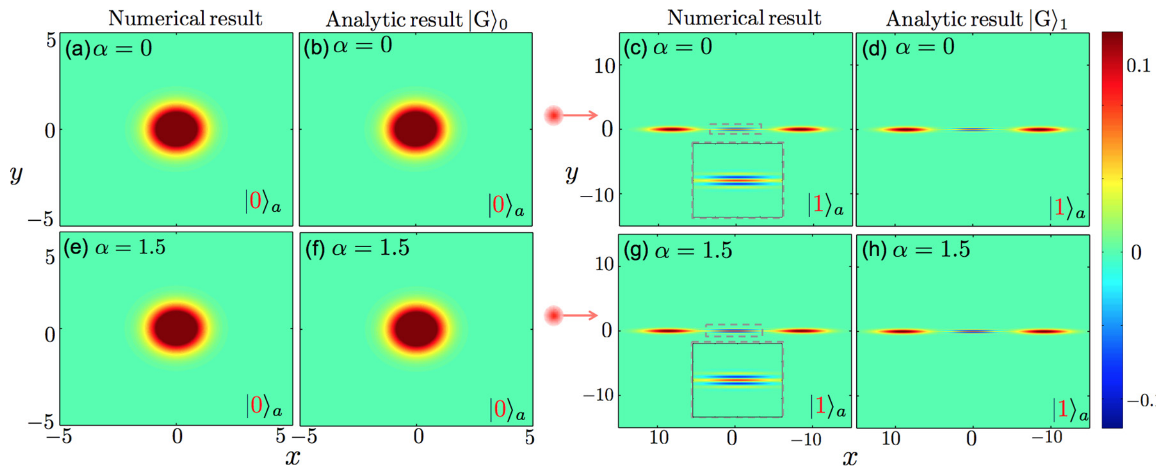

FIG. 5. The Wigner function of the reduced density matrix ρ_b when (a)–(d) $\alpha = 0$ and (e)–(h) $\alpha = 1.5$. The quadrature variables are $x = (b + b^\dagger)/2$ and $y = -i(b - b^\dagger)/2$. Corresponding to (a), (e), (c), and (g), ρ_b is obtained by diagonalizing the system Hamiltonian numerically and tracing out the qubit degree of freedom. (b), (f) and (d), (h) correspond to the approximate analytic ground state $|G\rangle_0$ and $|G\rangle_1$, respectively. The insets of (c) and (g) present the interference fringe of the cat state. The system parameters are the same as in Fig. 2 except for the value of χ corresponding to the blue dots of Fig. 4.

value of Ω/ω_n (see the bar graphs in Fig. 2). This leads to the result that, choosing the same value of Ω/ω, the case of $n = 1$ can be closer to the $\Omega/\omega_n \to \infty$ limit, where the QPT occurs exactly. Here, the results of finite Ω/ω are obtained by numerically diagonalizing Hamiltonian (2) in a large Hilbert space consisting of 1000 base vectors, and considering the squeezing transformation between modes b and b_n. This Hilbert space also has been used in the following numerical calculations.

IV. SINGLE-PHOTON-INDUCED ENTANGLEMENT AND QUANTUM SUPERPOSITION

Figures 2 and 3 also show the approximate occurrence of superradiant QPT induced by a single photon in the finite Ω/ω, which leads to single-photon-induced entanglement and quantum superposition.

Qualitatively, when the ancillary mode a is in the vacuum state $|0\rangle_a$, Hamiltonian (2) is reduced to a standard Rabi Hamiltonian. Under the conditions of $e^{-2r_1} < \chi \ll 1$ and $\Omega \approx \omega$, the ground state of the system is approximately $|G\rangle_0 = |0\rangle_b|\downarrow\rangle$, which is neither an entangled state nor a quantum superposition state. When the mode a is in the single-photon Fock state $|1\rangle_a$, the frequency ratio $\Omega/\omega_n \gg 1$ (see the bar graphs in Fig. 2), which allows the approximate occurrence of superradiant QPT when $\chi > e^{-2r_1}$. Correspondingly, the ground state of the system approximately becomes $|G\rangle_1 = (1/\sqrt{2})(|G\rangle_{\rm sp}^+ + |G\rangle_{\rm sp}^-)$ when $\chi > e^{-2r_1}$, which is a qubit-cavity entangled state. Moreover, from the ground state $|G\rangle_1$, we also could obtain the quantum superposition of the field b. One could measure the qubit in the $(|\downarrow\rangle_+ \pm |\downarrow\rangle_-)/\sqrt{2}$ basis (the definition of $|\downarrow\rangle_\pm$ is shown in the Appendix). Depending on the outcome of the measurement, the state of the field b is approximately projected into one of the following squeezed cat states,

$$|\Psi\rangle_1^{\rm sup} = \frac{1}{\sqrt{2}} S(\tilde{r}_{\rm tot})[D(|\beta|)|0\rangle_b \pm D(-|\beta|)|0\rangle_b]. \quad (3)$$

Quantitatively, to show the above single-photon-induced quantum entanglement more clearly, we numerically calculate the von Neumann entropy $S = -{\rm tr}(\rho_b \log_2 \rho_b)$ of the reduced density matrix ρ_b of the field mode, and present the dependence of S on χ in Fig. 4. It is shown that strong qubit-field quantum entanglement is triggered by injecting a single photon into the ancillary cavity, i.e., $|0\rangle_a \to |1\rangle_a$. This single-photon-induced quantum entanglement is immune to the A^2 term [see Fig. 4(b)]. Moreover, this strong qubit-field entanglement could be realized in a relatively weak-coupling regime, i.e., $\chi \ll 1$. However, in the normal Rabi model (see the case of $n = 0$ corresponding to the black solid lines in Fig. 4), the realization of strong qubit-field entanglement requires an ultrastrong-coupling regime $\chi > 1$ and ignoring the A^2 term.

To show single-photon-induced quantum superposition, in Fig. 5, we present the Wigner function of the reduced density matrices ρ_b with the numerical results and the approximate analytic ground states $|G\rangle_0, |G\rangle_1$, respectively. First of all, it clearly presents that the single-photon-induced quantum superposition can be realized both in the cases of ignoring and including the A^2 term. Here, the quantum superposition state is actually a squeezed cat state, as shown in Figs. 5(c), 5(d), 5(g), and 5(h). Second, comparing the exactly numerical results [i.e., Figs. 5(a) and 5(e) and Figs. 5(c) and 5(g)] with the analytic results [i.e., Figs. 5(b) and 5(f) and Figs. 5(d) and 5(h)], it is shown that the analytic ground states $|G\rangle_0$ and $|G\rangle_1$ can represent the system ground states with high fidelity. Then one could obtain a squeezed cat state $|\Psi\rangle_1^{\rm sup}$ with high fidelity after doing the qubit measurement into the ground state of system $|G\rangle_1$.

V. CONCLUSIONS

In conclusion, we have proposed a hybrid quantum model, which is equivalent to a photon-dependent Rabi model. Interestingly, this hybrid quantum model allows for the occurrence of single-photon-induced entanglement and quantum superposition. We also showed that these single-photon-induced quantum properties will not be limited by the so-called A^2 term. Moreover, here, the obtained quantum superposition state induced by a single photon actually is a squeezed cat state, which has potential applications in quantum metrology [46]. This work may offer the prospect of exploring the single-photon-induced ground-state quantum property together with its applications in high-precision single-photon quantum technologies.

Note added. Recently, two related works by Clerk's group [48] and Nori's group [53] appeared.

ACKNOWLEDGMENT

This work is supported by the National Key R&D Program of China (Grant No. 2016YFA0301203) and the National Science Foundation of China (Grants No. 11374116, No. 11574104, and No. 11375067).

APPENDIX: DIAGONALIZATION PROCEDURE OF HAMILTONIAN (2)

According to the diagonalization procedure used in Ref. [10], we can diagonalize Hamiltonian (2) in the $\Omega/\omega_n \to \infty$ limit (corresponding to the $\Omega/\omega \to \infty$ limit in terms of the original system parameters).

Specifically, when $\chi < \exp(-2r_n)$ (corresponding to the NP), Hamiltonian (2) can be diagonalized according to the following procedure. Applying a unitary transformation $U^\dagger H_n U$ with

$$U = \exp(S) = \exp\left[\frac{\lambda_n}{\Omega}(b_n + b_n^\dagger)(\sigma_+ - \sigma_-)\right], \tag{A1}$$

we obtain

$$H_n' = U^\dagger H_n U = \sum_{j=0}^{\infty} \frac{1}{j!}[H_n,S]^{(j)}, \tag{A2}$$

where the commutation rule is defined as $[H_n,S]^{(j)} \equiv [[H_n,S]^{(j-1)},S]$ with $[H_n,S]^{(0)} = H_n$. Expanding Eq. (A2), we can obtain

$$\begin{aligned} H' =& \frac{\Omega}{2}\sigma_z + \omega_n b^\dagger b + \frac{\chi_n^2\omega_n}{4}(b_n^\dagger + b_n)^2\sigma_z + C_n \\ &+ \frac{\chi_n\omega_n}{2}\sqrt{\frac{\omega_n}{\Omega}}(b_n^\dagger - b_n)(\sigma_+ - \sigma_-) \\ &+ \frac{\chi_n^3\omega_n}{6}\sqrt{\frac{\omega_n}{\Omega}}(b_n + b_n^\dagger)^3\sigma_x + O\left(\sqrt{\frac{\omega_n}{\Omega}}\right), \end{aligned} \tag{A3}$$

where the last term denotes the high-order terms of $\sqrt{\omega_n/\Omega}$. In the limit $\Omega/\omega_n \to \infty$ (originally from $\Omega/\omega \to \infty$), the fifth and sixth terms of Eq. (A3) and the high-order terms of $\sqrt{\omega_n/\Omega}$ [i.e., the last term of Eq. (A3)] become zero. Then, projecting the Hamiltonian into the spin-down subspace, the system Hamiltonian becomes

$$H_{\rm np} = \omega_n b_n^\dagger b_n - \frac{\chi_n^2\omega_n}{4}(b_n^\dagger + b_n)^2 - \frac{\Omega}{2} + C_n. \tag{A4}$$

This Hamiltonian could be diagonalized to $H_{\rm np} = \omega_e e^\dagger e + E_g$ by a squeezing transformation $b_n = e\cosh(l) + e^\dagger\sinh(l)$ with a squeezing parameter $l = -(1/4)\ln(1-\chi_n^2)$. Here, the excitation energy ω_e and the ground-state energy E_g are given by

$$\omega_e = \omega_n\sqrt{1-\chi_n^2}, \tag{A5a}$$

$$E_g = \frac{\omega_n}{2}\left(\sqrt{1-\chi_n^2} - 1\right) - \frac{\Omega}{2} + C_n. \tag{A5b}$$

The corresponding ground state of the system is $|G\rangle_{\rm np} = S(r_{\rm tot})|0\rangle_b|\downarrow\rangle$ with $S(r_{\rm tot}) = \exp[r_{\rm tot}(b^{\dagger 2} - b^2)/2]$ and $r_{\rm tot} = r_n + l$. This ground state has a conserved $\mathbb{Z}_2$ symmetry (i.e., $\Pi|G\rangle_{\rm np} = |G\rangle_{\rm np}$), confirmed by the zero ground-state coherence of field $\langle b\rangle_g = 0$.

The excitation energy ω_e is real only for $\chi \leqslant \exp(-2r_n)$ (corresponding to $\chi_n \leqslant 1$) and vanishes when $\chi = \exp(-2r_n)$, locating the occurrence of superradiant QPT. When $\chi > \exp(-2r_n)$, the system enters into the SP, and Eq. (A4) becomes invalid due to the field b_n being macroscopically occupied (being proportional to Ω/ω_n). In this case, we first displace the field mode b_n with an amplitude $\beta = \pm\sqrt{\frac{\Omega}{4\omega_n}(\chi_n^2 - \chi_n^{-2})}$ (i.e., $b_n \to \tilde{b}_n + \beta$), and then the system Hamiltonian becomes

$$\tilde{H}_n = \omega_n \tilde{b}_n^\dagger \tilde{b}_n + \frac{\tilde{\Omega}}{2}\tilde{\sigma}_z - \tilde{\lambda}(\tilde{b}_n^\dagger + \tilde{b}_n)\tilde{\sigma}_x + \omega_n\beta^2 + C_n, \tag{A6}$$

where the rescaled system coefficients $\tilde{\Omega} = \chi_n^2\Omega$, $\tilde{\lambda} = \sqrt{\Omega\omega_n}/(2\chi_n)$. Here, $\tilde{\sigma}_z$,$\tilde{\sigma}_x$ are the redefined Pauli operators in the rotated spin eigenstates given by

$$|\tilde{\downarrow}\rangle = \cos\theta|\downarrow\rangle - \sin\theta|\uparrow\rangle, \tag{A7a}$$

$$|\tilde{\uparrow}\rangle = \sin\theta|\downarrow\rangle + \cos\theta|\uparrow\rangle, \tag{A7b}$$

and $\tan(2\theta) = -4\lambda_n\beta/\Omega$. Note that Hamiltonian (A6) has the same formation as Hamiltonian (2). Then, by employing a similar procedure used to derive $H_{\rm np}$, Hamiltonian (A6) can be diagonalized to $H_{\rm sp} = \tilde{\omega}_e \tilde{e}^\dagger \tilde{e} + \tilde{E}_g$ with

$$\tilde{\omega}_e = \omega_n\sqrt{1-\chi_n^{-4}}, \tag{A8a}$$

$$\tilde{E}_g = \frac{\omega_n}{2}\left(\sqrt{1-\chi_n^{-4}} - 1\right) - \frac{\Omega}{4}\left(\chi_n^2 + \chi_n^{-2}\right) + C_n. \tag{A8b}$$

Here, the introduced operator $\tilde{e}$ is decided by a squeezing transformation $\tilde{e} = \tilde{b}_n\cosh(\tilde{l}) - \tilde{b}_n^\dagger\sinh(\tilde{l})$ with a squeezing parameter $\tilde{l} = -(1/4)\ln(1-\chi_n^{-4})$. Now, the ground state of the system becomes twofold degenerate given by $|G\rangle_{\rm sp}^{\pm} = D_n(\pm|\beta|)S(\tilde{r}_{\rm tot})|0\rangle_b|\downarrow\rangle_{\pm}$ with $D_n(\beta) = \exp(\beta b_n^\dagger - \beta_r^* b_n)$, $\tilde{r}_{\rm tot} = r_n + \tilde{l}$, and the spin states $|\downarrow\rangle_{\pm}$ given by

$$|\downarrow\rangle_{\pm} = \frac{\sqrt{1+\chi_n^{-2}}}{2}|\downarrow\rangle \pm \frac{\sqrt{1-\chi_n^{-2}}}{2}|\uparrow\rangle. \tag{A9}$$

Consequently, the $\mathbb{Z}_2$ symmetry of this ground state is spontaneously broken (i.e., $\Pi|G\rangle_{\rm sp}^{+} = |G\rangle_{\rm sp}^{-}$), confirmed by the nonzero ground-state coherence of field $\langle b\rangle_g^{\pm} = \pm e^{r_n}|\beta|$.

To characterize this superradiant QPT more clearly, the rescaled ground-state occupation of field b could be defined as the order parameter, i.e., $\psi_{\rm q} = [e^{-4r_n}\omega/\Omega]\langle b^\dagger b\rangle_g$. Based on the obtained ground state in the normal phase $|G\rangle_{\rm np}$ and the superradiant phase $|G\rangle_{\rm sp}^{\pm}$, we analytically calculate this order parameter, and obtain that $\psi_q = 0$ for $\chi < \exp(-2r_n)$ (corresponding to the NP) and $\psi_q = (1/4)(\chi_n^2 - \chi_n^{-2})$ becomes finite for $\chi > \exp(-2r_n)$ (corresponding to the SP). This property ensures the validity of the defined ψ_q as an order parameter for characterizing the QPT.

[1] S. L. Braunstein and P. V. Loock, Rev. Mod. Phys. **77**, 513 (2005).

[2] R. Horodecki, P. Horodecki, M. Horodecki, and K. Horodecki, Rev. Mod. Phys. **81**, 865 (2009).

[3] T. J. Osborne and M. A. Nielsen, Phys. Rev. A **66**, 032110 (2002).

[4] A. Osterloh, L. Amico, G. Falci, and R. Fazio, Nature (London) **416**, 608 (2002).

[5] G. Vidal, J. I. Latorre, E. Rico, and A. Kitaev, Phys. Rev. Lett. **90**, 227902 (2003).

[6] N. Lambert, C. Emary, and T. Brandes, Phys. Rev. Lett. **92**, 073602 (2004).

[7] N. Lambert, C. Emary, and T. Brandes, Phys. Rev. A **71**, 053804 (2005).

[8] S. Ashhab and F. Nori, Phys. Rev. A **81**, 042311 (2010).

[9] K. Hepp and E. H. Lieb, Ann. Phys. **76**, 360 (1973); Y. K. Wang and F. T. Hioe, Phys. Rev. A **7**, 831 (1973).

[10] M.-J. Hwang, R. Puebla, and M. B. Plenio, Phys. Rev. Lett. **115**, 180404 (2015).

[11] M. Liu, S. Chesi, Z.-J. Ying, X. Chen, H.-G. Luo, and H.-Q. Lin, Phys. Rev. Lett. **119**, 220601 (2017).

[12] K. Rzazewski, K. Wodkiewicz, and W. Zakowicz, Phys. Rev. Lett. **35**, 432 (1975).

[13] J. M. Knight, Y. Aharonov, and G. T. C. Hsieh, Phys. Rev. A **17**, 1454 (1978).

[14] P. Nataf and C. Ciuti, Nat. Commun. **1**, 72 (2010).

[15] O. Viehmann, J. von Delft, and F. Marquardt, Phys. Rev. Lett. **107**, 113602 (2011).

[16] S. De Liberato, Phys. Rev. Lett. **112**, 016401 (2014).

[17] A. Vukics, T. Grießer, and P. Domokos, Phys. Rev. Lett. **112**, 073601 (2014).

[18] T. Jaako, Z. L. Xiang, J. J. Garcia-Ripoll, and P. Rabl, Phys. Rev. A **94**, 033850 (2016).

[19] K. M. Birnbaum, A. Boca, R. Miller, A. D. Boozer, T. E. Northup, and H. J. Kimble, Nature (London) **436**, 87 (2005).

[20] T. Peyronel, O. Firstenberg, Q.-Y. Liang, S. Hofferberth, A. V. Gorshkov, T. Pohl, M. D. Lukin, and V. Vuletić, Nature (London) **488**, 57 (2012).

[21] C. Santori, D. Fattal, J. Vuckovic, G. S. Solomon, and Y. Yamamoto, Nature (London) **419**, 594 (2002).

[22] S. V. Polyakov, A. Muller, E. B. Flagg, A. Ling, N. Borjemscaia, E. Van Keuren, A. Migdall, and G. S. Solomon, Phys. Rev. Lett. **107**, 157402 (2011).

[23] J. H. Prechtel, A. V. Kuhlmann, J. Houel, L. Greuter, A. Ludwig, D. Reuter, A. D. Wieck, and R. J. Warburton, Phys. Rev. X **3**, 041006 (2013).

[24] J. E. Kennard, J. P. Hadden, L. Marseglia, I. Aharonovich, S. Castelletto, B. R. Patton, A. Politi, J. C. F. Matthews, A. G. Sinclair, B. C. Gibson, S. Prawer, J. G. Rarity, and J. L. O'Brien, Phys. Rev. Lett. **111**, 213603 (2013).

[25] M. Pechal, L. Huthmacher, C. Eichler, S. Zeytinoğlu, A. A. Abdumalikov, Jr., S. Berger, A. Wallraff, and S. Filipp, Phys. Rev. X **4**, 041010 (2014).

[26] C. Hempel, B. P. Lanyon, P. Jurcevic, R. Gerritsma, R. Blatt, and C. F. Roos, Nat. Photon. **7**, 630 (2013).

[27] P. Grangier, J. A. Levenson, and J. Poizat, Nature (London) **396**, 537 (1998).

[28] M. D. Lukin and A. Imamoglu, Phys. Rev. Lett. **84**, 1419 (2000).

[29] K. Xia, M. Johnsson, P. L. Knight, and J. Twamley, Phys. Rev. Lett. **116**, 023601 (2016).

[30] E. Knill, R. Laflamme, and G. Milburn, Nature (London) **409**, 46 (2001).

[31] L. Neumeier, M. Leib, and M. J. Hartmann, Phys. Rev. Lett. **111**, 063601 (2013).

[32] L. Zhou, L.-P. Yang, Y. Li, and C. P. Sun, Phys. Rev. Lett. **111**, 103604 (2013).

[33] S. Baur, D. Tiarks, G. Rempe, and S. Dürr, Phys. Rev. Lett. **112**, 073901 (2014).

[34] I. Söllner, L. Midolo, and P. Lodahl, Phys. Rev. Lett. **116**, 234301 (2016).

[35] M. Aspelmeyer, T. J. Kippenberg, and F. Marquardt, Rev. Mod. Phys. **86**, 1391 (2014).

[36] H. Xiong, L.-G. Si, X.-Y. Lü, X.-X. Yang, and Y. Wu, Sci. China Phys. Mech. Astron. **58**, 1 (2015).

[37] X.-Y. Lü, Y. Wu, J. R. Johansson, H. Jing, J. Zhang, and F. Nori, Phys. Rev. Lett. **114**, 093602 (2015).

[38] X.-Y. Lü, H. Jing, J.-Y. Ma, and Y. Wu, Phys. Rev. Lett. **114**, 253601 (2015).

[39] J. D. Thompson, B. M. Zwickl, A. M. Jayich, F. Marquardt, S. M. Girvin, and J. G. E. Harris, Nature (London) **452**, 72 (2008).

[40] M. Bhattacharya, H. Uys, and P. Meystre, Phys. Rev. A **77**, 033819 (2008).

[41] J.-Q. Liao and F. Nori, Phys. Rev. A **88**, 023853 (2013).

[42] M. R. Vanner, Phys. Rev. X **1**, 021011 (2011).

[43] H. K. Li, Y.-C. Liu, X. Yi, C.-L. Zou, X.-X. Ren, and Y.-F. Xiao, Phys. Rev. A **85**, 053832 (2012).

[44] E. J. Kim, J. R. Johansson, and F. Nori, Phys. Rev. A **91**, 033835 (2015).

[45] M. Cirio, K. Debnath, N. Lambert, and F. Nori, Phys. Rev. Lett. **119**, 053601 (2017).

[46] H.-Y. Lo, D. Kienzler, L. de Clercq, M. Marinelli, V. Negnevitsky, B. C. Keitch, and J. P. Home, Nature (London) **521**, 336 (2015).

[47] P. A. Knott, T. J. Proctor, A. J. Hayes, J. P. Cooling, and J. A. Dunningham, Phys. Rev. A **93**, 033859 (2016).

[48] C. Leroux, L. C. G. Govia, and A. A. Clerk, Phys. Rev. Lett. **120**, 093602 (2018).

[49] Z.-L. Xiang, S. Ashhab, J. Q. You, and F. Nori, Rev. Mod. Phys. **85**, 623 (2013).

[50] F. Dimer, B. Estienne, A. S. Parkins, and H. J. Carmichael, Phys. Rev. A **75**, 013804 (2007).

[51] K. Baumann, C. Guerlin, F. Brennecke, and T. Esslinger, Nature (London) **464**, 1301 (2010).

[52] M. P. Baden, K. J. Arnold, A. L. Grimsmo, S. Parkins, and M. D. Barrett, Phys. Rev. Lett. **113**, 020408 (2014).

[53] W. Qin, A. Miranowicz, P.-B. Li, X.-Y. Lü, J.-Q. You, and F. Nori, Phys. Rev. Lett. **120**, 093601 (2018).